

Auger decay in the field of a positive charge

Vitali Averbukh,^{1,*} Ulf Saalmann,^{1,2} and Jan Michael Rost^{1,2}

¹Max Planck Institute for the Physics of Complex Systems, Nöthnitzer Straße 38, 01187 Dresden, Germany

²Max Planck Advanced Study Group at CFEL, Luruper Chaussee 149, 22761 Hamburg, Germany

(Received 15 October 2011; revised manuscript received 18 May 2012; published 6 June 2012)

We consider the Auger decay of atomic inner-shell vacancies in the field of a positive charge, as it occurs in multiply ionized molecules and clusters in strong x-ray laser pulses. First-principles numerical calculations of the decay rate as a function of the ion-charge distance are presented for a series of Auger transitions. The dependence of the rate on the distance is analyzed qualitatively within the Wentzel theory. Our results show that Auger rates can be modified significantly at ion-charge distances of the order of chemical bond lengths. The origin of the predicted effect is traced back to the distortion of the valence orbitals by the field of the positive charge.

DOI: [10.1103/PhysRevA.85.063405](https://doi.org/10.1103/PhysRevA.85.063405)

PACS number(s): 32.80.Aa, 32.80.Hd, 36.40.Wa, 41.60.Cr

I. INTRODUCTION

Auger processes [1], as sketched in Fig. 1, are a general consequence of the interaction of x-ray radiation with matter and, as such, are one of the key elements in the mechanisms of radiation damage, e.g., in biomolecules (see, for example, the discussion in Ref. [2] and references therein). In the conventional x-ray diffraction spectroscopy of molecular crystals, the radiation damage is an important consideration which puts limits on the intensity of the incident x-ray beam. In the proposed modern applications of the high-intensity x-ray free electron lasers (XFELs) [3] to perform single-species x-ray diffraction from macromolecules [4,5], radiation damage is of paramount importance to the mere feasibility of the discussed idea. Here, the expected role of the Auger processes is rather intriguing. On the one hand, Auger decay of the *K*-shell vacancies of carbon, oxygen, and nitrogen atoms contributes directly to the accumulation of the positive charge and eventually to the molecular decomposition. Moreover, the emitted Auger electrons can interact with the bound molecular electrons leading to further multiple ionization by electron impact cascades [6]. On the other hand, however, filling of the *K*-shell vacancies by Auger decays contributes to the formation of the molecular diffraction picture, because it is the x-ray scattering from the localized electrons that gives us information about the atomic positions [7].

While the exact role of the Auger decay in single-molecule x-ray diffraction is yet to be understood, it is already clear that most of the XFEL-induced Auger events occur in the field of (multiple) positive charges. Indeed, theoretical simulations of molecular [4,7] and cluster [8] decomposition in the XFEL field show that the polyatomic species become multiply ionized well within the XFEL pulse duration. Two important aspects make Auger transition in such multiply ionized systems different from the ones in free atoms. First, Auger electron trapping changes the dynamics of the core hole decay qualitatively from an exponential to an oscillatory one [9]. Second, the rate of the exponential decay in the field of the positive charges does not have to match the one

in the singly core-ionized molecule. While the suppression of the exponential decay due to Auger electron trapping was considered by us in a recent work [9], the problem of exponential Auger decay in the field of the positive charges has not been given attention so far. Here we present a study of the most basic problem of this kind, namely we investigate atomic Auger effect in the field of a single stationary positive charge (a proton). The questions we are asking are the following. What is the behavior of the Auger rate as a function of the atom-charge distance? And how big is the change in the atomic Auger rate at the atom-charge distances characteristic of interatomic separations in molecules and clusters?

The paper is organized as follows. In the next section we discuss the effect of a neighboring point charge on the atomic Auger rate qualitatively within the Wentzel theory. Our results for a series of Auger decay rates in atom-proton systems obtained by the Fano-ADC *ab initio* method are presented and analyzed in Sec. III. Section IV is devoted to conclusions.

II. RATE OF AUGER DECAY IN THE FIELD OF A POSITIVE CHARGE: QUALITATIVE CONSIDERATIONS

The first theory of Auger effect was given by Wentzel in his seminal work on the nonradiative quantum jumps [10]. Wentzel used hydrogenic bound-state functions and the asymptotic forms of the free electron waves to predict the order of magnitude of an electronic decay rate in a two-electron system. Adapted to a single Auger decay channel leading to a singlet final state of the dication of the kind shown in Fig. 1, Wentzel's expression becomes

$$\Gamma = \pi \left\langle \left\langle \varphi_{\text{val}}(\vec{r}_1) \varphi'_{\text{val}}(\vec{r}_2) \left| \frac{1}{r_{12}} \right| \varphi_{\text{core}}(\vec{r}_1) \varphi_{\varepsilon}(\vec{r}_2) \right\rangle \right\rangle + \left\langle \left\langle \varphi_{\text{val}}(\vec{r}_1) \varphi'_{\text{val}}(\vec{r}_2) \left| \frac{1}{r_{12}} \right| \varphi_{\text{core}}(\vec{r}_2) \varphi_{\varepsilon}(\vec{r}_1) \right\rangle \right\rangle^2. \quad (1)$$

It embodies the idea that one of the electrons participating in the Auger transition “jumps” from a valence orbital, φ_{val} , to the core orbital, φ_{core} , while the second electron is ejected from another valence orbital, φ'_{val} , to the continuum with the kinetic energy ε (compare to Fig. 1). Electron indistinguishability leads to two interfering pathways for such a jump, often called “direct” and “exchange”. Despite the strong approximations

*Present address: Department of Physics, Imperial College London, Prince Consort Road, London SW7 2AZ, United Kingdom; v.averbukh@imperial.ac.uk

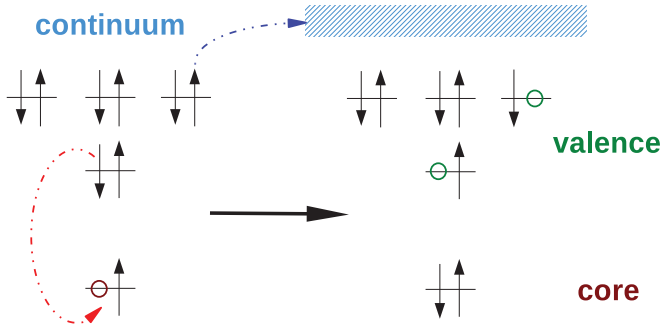


FIG. 1. (Color online) Schematic representation of one of the channels of the $1s$ Auger decay in Ne atom: an inner valence ($2s$) electron is filling the core vacancy, while an outer valence ($2p$) electron is ejected into continuum. The same final state results also from the $2p \rightarrow 1s$ recombination and $2s$ ionization (not shown here). The former (“direct”) and the latter (“exchange”) contributions interfere due to electron indistinguishability.

used in Wentzel’s original theory (e.g., use of very approximate electronic orbitals), it does predict the order of magnitude of the Auger rate rather well (1 fs^{-1} , to be compared with 0.1 to 0.5 fs^{-1} for the K -shell Auger of first row elements [11]). Here we shall use Wentzel’s expression (1) for the qualitative analysis of the effect of a neighboring charge on the Auger rate.

Suppose an Auger transition occurs in the field of a stationary point charge being at the distance R from the core-ionized atom, R being of the order of 1 \AA or bigger. In such a case, Wentzel’s formula (1) suggests that the Auger rate can be influenced by the charge through the distortions of the electronic orbitals participating in the transition. The tightly bound core orbital, φ_{core} , is not likely to be affected, since its binding energy is typically at least an order of magnitude higher than interaction energy of the core electron with a unit charge at 1 \AA distance. Typical kinetic energy of an Auger electron is also much higher than its interaction energy with the point charge. A visible effect of the charge on the Auger rate (1) can come, nevertheless, through distortion of the valence orbitals, $\varphi_{\text{val}}, \varphi'_{\text{val}}$, especially if the latter are easily polarizable. Indeed, binding energies of atomic valence orbitals ranging from $\sim 3.9 \text{ eV}$ to $\sim 24.6 \text{ eV}$ are of the same order of magnitude as the electron-proton attraction at the distance of 1 \AA ($\sim 14.4 \text{ eV}$).

Let us look closer at the possible effect of the point charge on the Auger rate bearing in mind the importance of the valence orbital distortion. To this end, we shall further simplify Wentzel’s expression (1) by neglecting exchange and representing the direct Auger transition matrix element as a repulsion energy between two charge clouds:

$$V_{\text{Auger}} = \int d^3 r_1 \int d^3 r_2 \varphi_{\text{val}}(\vec{r}_1) \varphi_{\text{core}}(\vec{r}_1) \frac{1}{r_{12}} \varphi'_{\text{val}}(\vec{r}_2) \varphi_{\varepsilon}(\vec{r}_2) \quad (2)$$

and using a multipole expansion [12] assuming $r_1 < r_2$

$$V_{\text{Auger}} = \sum_{l,m} \frac{4\pi}{2l+1} \langle \varphi_{\text{val}}(\vec{r}_1) | r_1^l Y_{lm}^*(\theta_1, \varphi_1) | \varphi_{\text{core}}(\vec{r}_1) \rangle \times \langle \varphi'_{\text{val}}(\vec{r}_2) | Y_{lm}(\theta_2, \varphi_2) / r_2^{l+1} | \varphi_{\varepsilon}(\vec{r}_2) \rangle, \quad (3)$$

where $Y_{lm}(\theta, \varphi)$ are spherical harmonics [12]. Effectively, the multipole expansion breaks the two-electron transition into a recombination and an ionization part. The lowest nonzero angular momentum contribution to the expansion (3) defines the multiplicity of the given Auger transition.

Following Bloch [13], one can perform a crude analysis of Eq. (3) using the spatial extension of the core orbital r_{core} and the valence orbitals r_{val} . Since typically $r_{\text{core}} \ll r_{\text{val}}$ the recombination matrix element scales as r_{core}^l . Accordingly, the ionization matrix element scales as $1/r_{\text{val}}^{l+1}$. Thus we obtain

$$V_{\text{Auger}} \sim r_{\text{core}}^l / r_{\text{val}}^{l+1}. \quad (4)$$

Practically, this scaling means that, in order to increase the Auger rate, one has to lower the multiplicity of the transition, l , and/or to contract the valence orbital. Both effects can be achieved through valence orbital distortion by the point charge. Indeed, at atom-proton distances larger than r_{val} one can expect orbital distortion to result in a symmetry lowering that naturally leads to a change in Auger transition multiplicity. At shorter distances, a proton penetrating the valence electron cloud would lead to an effective r_{val} smaller than that in a free system. In what follows, we shall explore these effects quantitatively using a first-principles description of the electronic decay.

III. AUGER DECAY RATES IN ION-PROTON SYSTEMS BY FANO-ADC METHOD

In all our Auger-width calculations we are using a Fano-ADC (algebraic diagrammatic construction) technique [14]. The Fano-ADC approach for electronic decay widths is an \mathcal{L}^2 method that is based on the Fano expression [15] for the decay width Γ through the matrix element of the full many-electron Hamiltonian \hat{H} between the boundlike (Φ) and the continuumlike ($\chi_{\alpha, \varepsilon_{\alpha}}$) components of the wave function at the energy of the resonance E_r :

$$\Gamma = 2\pi \sum_{\alpha=1}^{N_c} |\langle \Phi | \hat{H} - E_r | \chi_{\alpha, \varepsilon_{\alpha}} \rangle|^2, \quad (5)$$

where the summation is over N_c decay channels and ε_{α} is the kinetic energy of the emitted electron for the α ’s decay channel. The many-electron wave functions Φ and $\chi_{\alpha, \varepsilon_{\alpha}}$ are obtained using the *ab initio* method known as extended second-order algebraic diagrammatic construction [ADC(2)x]. In the case of the Auger decay of singly ionized states, an ADC(2)x scheme for $N-1$ electron systems is employed [16], N standing for the number of electrons in the closed shell ground state of neutral species. Finally, the interpolation and renormalization of the bound-continuum matrix elements obtained with \mathcal{L}^2 wave functions is achieved by Stieltjes imaging procedure [17]. In the center of the Fano-ADC computational procedure is the configuration selection scheme that sorts out the many-electron ADC basis states into those contributing to the expansion of the initial (boundlike) state and to the final (continuumlike) state. In all the calculations performed in this study, we employ the energy-based configuration selection scheme [14] in which the initial state of the decay has been chosen as the state with the maximal overlap with the core-ionized configuration. Such initial state corresponds to the atomic core-ionized state

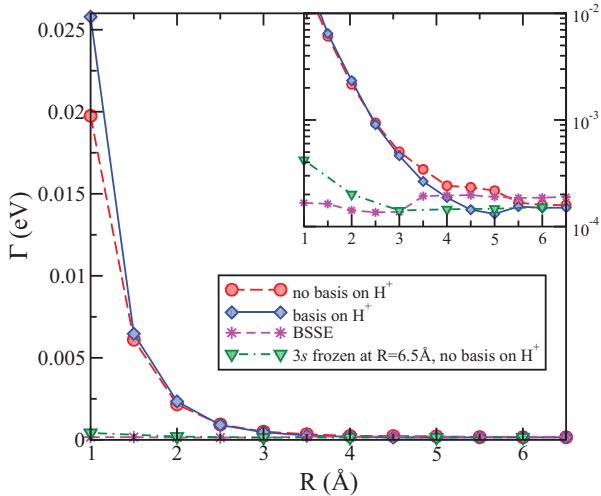


FIG. 2. (Color online) Auger decay width of $(2p_z^{-1})\text{Mg}^+-\text{H}^+$ Fano-ADC(2)x calculations as a function of the Mg-proton distance R with z the Mg-proton axis. Diamonds and solid line: atomic orbital basis centered both on Mg and on the proton; circles and long-dashed line: atomic orbital basis centered only on Mg; stars and short-dashed line: calculation for $(2p_z^{-1})\text{Mg}^+$ alone, with atomic orbital basis centered both on Mg and at the distance R along the z axis, showing the so-called basis set superposition error (BSSE); triangles and dashed-dotted line: atomic orbital basis centered on Mg only, with the $3s$ orbital of Mg being frozen at its shape at $R = 6.5 \text{ \AA}$. The inset shows the low- Γ part of the plot on logarithmic scale.

in the separated atom limit. Thus, if the core-ionized potential energy curve (PEC) of atom-proton system ($X^{+*}-\text{H}^+$, X is an atom) undergoes an avoided crossing, e.g., with a core-valence ionized PEC of the $X^{2+}-\text{H}$ type [18], the resulting Fano-ADC decay width corresponds to the diabatic $X^{+*}-\text{H}^+$ state. The effects of the avoided crossings on the Auger widths of the adiabatic core-ionized states are very system-specific and are beyond the scope of the present work. Prerequisite for the ADC calculations is the restricted Hartree-Fock (RHF) solution of the corresponding N -electron system. In the present work, the molecular RHF calculations for the $X-\text{H}^+$ systems were performed using the MOLCAS6 quantum chemistry package [19].

A. Single-channel decay

Let us first consider a simple Auger process with only a single decay channel [$N_c = 1$ in Eq. (5)]. While not characteristic of K -shell Auger, such processes take place upon $(n-1)p$ ionization of alkaline earth atoms, e.g., in $(2p^{-1})\text{Mg}^+$, where the only nonradiative decay pathway involves the two $3s$ electrons: $(2p^{-1})\text{Mg}^+ \rightarrow (3s^{-2})\text{Mg}^{2+} + e^-$. Assume that $(2p^{-1})\text{Mg}^+$ Auger decay occurs in the field of a stationary positive charge, say, of a proton fixed at the distance R from the Mg^+ ion. Then, following the arguments of Sec. II, we should expect the decay width Γ to vary as a function of R due to distortion of the valence $3s$ orbital. In Fig. 2 we present the results of our Fano-ADC(2)x calculations for the $\Gamma(R)$ in the $(2p^{-1})\text{Mg}^+-\text{H}^+$ system that indeed reveals such a variation. Here and later on we use atomic rather than molecular notation for the core-ionized states of atom-proton

systems in order to make clear the correspondence to the separated atom limit and to underscore the fact that the presented decay width corresponds to diabatic states of the $X^{+*}-\text{H}^+$ type.

The Gaussian orbital basis set used in these calculations was the uncontracted cc-pCVQZ basis (all the standard Gaussian bases used in this work have been obtained from the EMSL database [20]) augmented by $3s3p3d$ diffuse Gaussians of Kaufmann-Baumeister-Jungen (KBJ) type [21] centered on Mg, an additional distributed Gaussian basis of $5s5p5d$ KBJ Gaussians centered at $(\pm 0.5 \text{ \AA}, 0, 0)$, $(0, \pm 0.5 \text{ \AA}, 0)$, $(0, 0, \pm 0.5 \text{ \AA})$, and $(\pm 0.5 \text{ \AA}, \pm 0.5 \text{ \AA}, \pm 0.5 \text{ \AA})$, where $(0, 0, 0)$ is the Mg position, and an uncontracted cc-PVQZ basis augmented by $3s3p$ KBJ Gaussians centered on the proton. At large Mg-proton separations, the calculated width converges to about 0.16 meV, in a good agreement with the theoretical value of 0.145 meV by Walters and Bhalla for the isolated Mg atom [22]. Our results show that, at the distances below 4 \AA , the decay width grows very strongly with decreasing Mg^+-H^+ distance. Practically the same result is obtained when removing the Gaussian basis from the proton, i.e., the possible transfer of Mg electron density to the neighboring charge does not play a key role in the effect (see Fig. 2). Moreover, the predicted increase of the decay width is not an artifact of the Gaussian basis set itself that, of course, also changes with R —this is verified by repeating the calculation in full Gaussian basis, but with zero charge on the “proton” (see line marked “BSSE” in Fig. 2). Finally, the clear indication that the predicted effect is due to the distortion of the valence orbital comes from another set of *ab initio* calculations, in which we “freeze” the Gaussian orbital coefficients in the Mg $3s$ orbital of $\text{Mg}-\text{H}^+$ at their values at the largest considered distance of $R = 6.5 \text{ \AA}$. The results presented in Fig. 2 show that the strong effect of the Auger width increase practically vanishes if the $3s$ orbital is frozen.

Further insight into the strong variation of the Auger decay width as a function of the Mg-proton distance is gained by the qualitative analysis in the spirit of Eqs. (3) and (4). Indeed, at $R \rightarrow \infty$ the $(2p^{-1})\text{Mg}^+$ Auger transition is of dipole-dipole type [$l = 1$; see Eq. (3)]. As the Mg-proton distance decreases, the Mg $3s$ orbital is distorted such that it attains a nonzero p_z component, reducing the multiplicity of the Auger transition to $l = 0$ and leading to the increase in the Auger width. This effect of the valence orbital distortion at $R > 2.5 \text{ \AA}$ is readily seen in the data presented in Fig. 3 [panels (a) and (b)]. As the proton approaches the Mg^+ ion further, it penetrates the valence electron orbital and eventually leads to its contraction; see Fig. 3(c). Thus, also at $R > 2.5 \text{ \AA}$, although the distortion of the $3s$ orbital along the Mg-proton axis decreases, the orbital contraction effect [quantified by the decrease of r_{val} , see Eq. (4)] leads to a further increase of the Auger rate.

B. Coster-Kronig decay

The above analysis suggests that the spectacular effect of the neighboring charge on the single-channel Mg $2p$ Auger decay has to do with the polarizable Mg $3s$ orbital that is involved in both the recombination and the ionization part of the two-electron transition. Let us consider now a more general situation, in which a polarizable orbital is involved only in the ejection of the Auger electron. An example of such

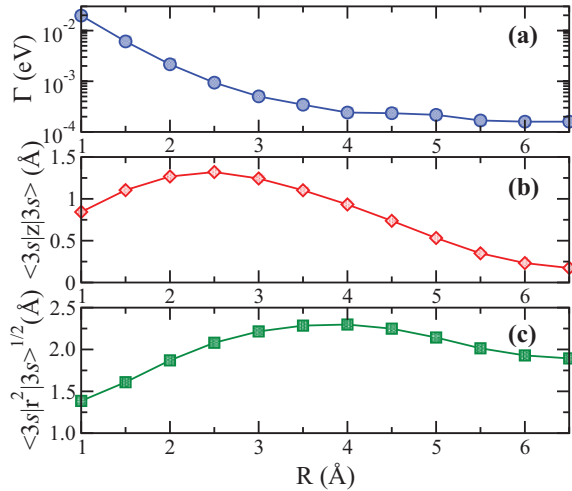


FIG. 3. (Color online) (a) Fano-ADC(2)x result for the Auger decay width of $(2p^{-1}) \text{Mg}^+-\text{H}^+$ as a function of the Mg-proton distance, R (logarithmic scale); (b) z expectation value of the Mg $3s$ orbital as a function of the Mg-proton distance, R , showing the extent of the orbital distortion along the Mg-proton axis; (c) mean radius of the Mg $3s$ orbital as a function of the Mg-proton distance, R , showing the spatial extent.

a transition is readily provided by $2s$ -ionized Mg. Indeed, $2s$ ionization leads to the process in which one of the $2p$ electrons fills the vacancy, while a $3s$ electron is ejected into continuum: $(2s^{-1}) \text{Mg}^+ \rightarrow (2p^{-1}3s^{-1}) \text{Mg}^{2+} + e^-$. This decay is characterized by the recombination transition occurring within a single ($n=2$) electronic shell and as such belongs to the class of Coster-Kronig (CK) decay processes. The efficient recombination part of the transition and the relatively low kinetic energies of the CK electrons contribute to the typically large widths of the CK decay. In the particular case of $(2s^{-1}) \text{Mg}^+$, the CK transition is by far the leading decay channel with the competing $(2s^{-1}) \text{Mg}^+ \rightarrow (3s^{-2}) \text{Mg}^{2+} + e^-$ Auger decay being much weaker.

Figure 4 shows the results of the Fano-ADC(2)x calculation of the $(2s^{-1}) \text{Mg}^+$ decay width in the Mg^+-H^+ system as a function of the Mg-proton distance. The decay is completely dominated by the CK process, accounting for 95%–99% of the total electronic decay width. At large R , the Fano-ADC(2)x result assuming no electron density on the proton is in excellent agreement with the R -matrix prediction for bare $(2s^{-1}) \text{Mg}^+$ [23]. We observe a well-pronounced dependence of the CK on the Mg-proton distance that is drastically reduced by artificially freezing the $3s$ orbital at its large- R shape. The increase of the decay width at small internuclear distances is easily attributable to the effect of the valence orbital contraction, as in the case of $(2p^{-1}) \text{Mg}^+$ decay. Analysis of the partial decay widths (not shown here) reveals that the behavior of the width at larger Mg-proton distances varies for different decay channels, e.g., singlet vs triplet final states, and thus cannot be explained by the simple arguments of Sec. II. The magnitude of the neighboring charge effect on the $(2s^{-1}) \text{Mg}^+$ transition is less than in the case of the $(2p^{-1}) \text{Mg}^+$ decay, apparently because the distorted valence orbital is only involved in the ionization part of the two-electron transition. Noteworthy is a clearly distinguishable effect that

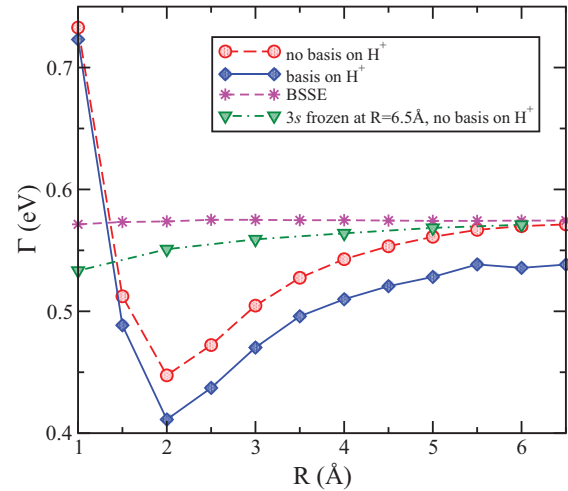


FIG. 4. (Color online) Decay width of $(2s^{-1}) \text{Mg}^+-\text{H}^+$ as a function of the Mg-proton distance, R . Diamonds and solid line: Fano-ADC(2)x calculation with atomic orbital basis centered both on Mg and on the proton; circles and long-dashed line: Fano-ADC(2)x calculation with atomic orbital basis centered only on Mg; stars and short-dashed line: BSSE (see Fig. 2); triangles and dashed-dotted line: Fano-ADC(2)x calculation with atomic orbital basis centered on Mg only, with the $3s$ orbital of Mg being frozen at its shape at $R = 6.5$ Å.

the electronic density on the proton has on the decay. Allowing part of the electronic density to reside on the proton diminishes the electronic density on the core ionization site and as a result leads to the reduction of the CK decay width (see Fig. 4). Assuming that the neighboring charge was formed long before an instantaneous Mg core ionization, the physical decay width is produced by the calculation with basis set on the proton. If, on the other hand, Mg and a neighboring site ionization occur closely in time on the scale of the CK lifetime, the dynamics of the neighboring hole should be taken into account. Such a hole dynamics induced by electron correlation can take place at fixed nuclear geometries on the time scales comparable to the ones of CK or Auger decay [24] and is expected to be strongly influenced by the nuclear motion, at least on a bit longer time scales. Consideration of this effect is out of the scope of the present work.

C. Multichannel decay

Let us finally consider the effect of a neighboring charge on an Auger transition lacking a single dominant decay channel. We have chosen $(2p^{-1}) \text{Ar}^+$ decay in the field of a proton as an example of such a process. In our Ar calculations we have used the uncontracted cc-pCVQZ basis augmented by $7s7p7d7f$ diffuse Gaussians of the KBJ type [21] and the uncontracted cc-pVQZ basis augmented by $6s6p6d$ KBJ Gaussians centered on the proton. The results of our calculations are presented in Fig. 5. At large R , the Fano-ADC(2)x result is in reasonable agreement with the recommended literature value for the $(2p^{-1}) \text{Ar}^+$ decay width of 0.13 eV [11]. At shorter Ar-proton distances, our calculation predicts a noticeable decrease of the decay width with the electron density transfer to the proton starting to contribute around $R = 3.5$ Å. This decrease,

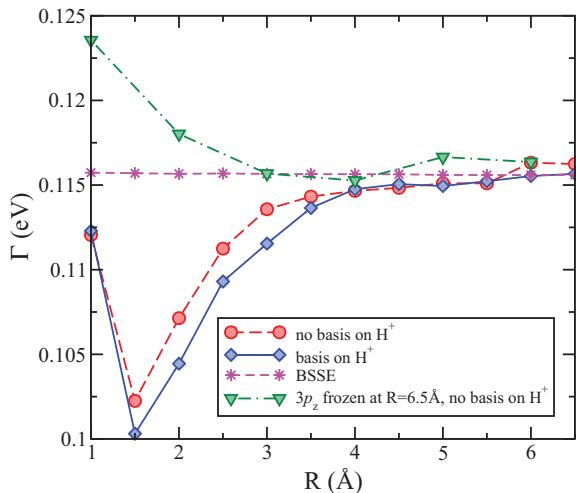


FIG. 5. (Color online) Decay width of $(2p_z^{-1}) \text{Ar}^+ - \text{H}^+$ as a function of the Ar-proton distance, R . Diamonds and solid line: Fano-ADC(2)x calculation with atomic orbital basis centered both on Ar and on the proton; circles and long-dashed line: Fano-ADC(2)x calculation with atomic orbital basis centered only on Ar; stars and short-dashed line: BSSE (see Fig. 2); triangles and dashed-dotted line: Fano-ADC(2)x calculation with atomic orbital basis centered on Ar only, with the $3p_z$ orbital of Ar being frozen at its shape at $R = 6.5 \text{ \AA}$.

however, cannot be traced to a change in a single atomic orbital and in fact results from a superposition of R dependences of several partial widths, such as $(3s^{-1}3p_z^{-1})^1\Sigma$, $(3s^{-1}3p_z^{-1})^3\Sigma$, $(3p_z^{-2})^1\Sigma$, $(3p_z^{-1}3p_{x,y}^{-1})^1\Pi$, and $(3p_z^{-1}3p_{x,y}^{-1})^3\Pi$. Although the outer valence orbital oriented along the Ar-proton axis, $3p_z$, is involved in all the major decay channels, freezing its shape at a large R does not lead to as strong a suppression of the R dependence of the total decay width as observed in the Mg results (see Figs. 2, 4, and 5). Obviously, this has to do with the distortion of the $3p_{x,y}$ orbitals by the field of the proton. At $R \leq 1.5 \text{ \AA}$ the contraction of the outer valence orbitals of Ar leads to amplification of the decay width for all the Auger channels and as a result to the increase of the total width as shown in Fig. 5.

IV. CONCLUSIONS

In conclusion, we have studied Auger decay widths in core-ionized atoms in the field of a point charge—a proton. Our *ab initio* Fano-ADC(2)x results for a number of Auger-type

transitions in Mg and Ar show a pronounced dependence of the Auger width on the atom-proton distance. The origin of this dependence is traced to the distortion of the outer valence atomic orbital by the field of the proton. A simple qualitative physical picture was given to explain the predicted dependence in terms of the change of multiplicity of Auger transitions and the valence orbital contraction as a result of the interaction with the proton. We have shown that the neighboring charge effect on the width of Auger decay can be dramatic if the same polarizable valence orbital is involved both in the recombination and in the ionization parts of the two-electron transition, as it is the case in $(2p^{-1}) \text{Mg}^+$ decay.

The magnitude of the predicted neighboring charge differs substantially between different Auger-type transitions, but is found to be the strongest at the atom-proton distances of about 1 to 2 \AA , i.e., at distances of the order of chemical bond length. At distances of 3 to 4 \AA , typical of interatomic distances in van der Waals clusters, the neighboring charge effect is much less pronounced. Thus we conclude that the use of atomic Auger rates in radiation damage simulations involving multiply ionized polyatomic molecules [4] is not *a priori* justified. Detailed analysis of the effect of the neighboring charges on Auger transitions in core-ionized organic and biomolecules will be a subject of future investigations. Nevertheless, our studies have already revealed a strong effect of an additional valence hole residing on the core-ionized carbon, nitrogen, or oxygen [25]. It would be also interesting to examine the neighboring charge effect on the rate of interatomic decay processes, such as interatomic Coulombic decay (ICD) in clusters [26]. This could provide additional insight into the dynamics of ICD in water solutions of ionic compounds [27]. Finally, while the present study targets the effect of a single neighboring charge, one could easily use the present computational method to describe a more general situation of the effect of several charges. Such computations should be feasible given that the main effect is expected to occur through distortion of the valence orbitals taking part in an Auger or ICD transition and thus can be characterized without considering the transfer of electron density to the neighboring charger, i.e., using modest basis sets.

ACKNOWLEDGMENTS

V.A. would like to acknowledge interesting discussions with J. Ullrich and R. Moshhammer and valuable help of V. Vysotskiy with *ab initio* computations.

-
- [1] W. Mehlhorn, in *Atomic Inner-Shell Physics*, edited by B. Crasemann (Plenum, New York, 1985).
 - [2] Ph. Bernhardt, W. Friedland and H. G. Paretzke, *Radiat. Environ. Biophys.* **43**, 77 (2004).
 - [3] J. Feldhaus, J. Arthur, and J. B. Hastings, *J. Phys. B* **38**, S799 (2005).
 - [4] R. Neutze, R. Wouts, D. van der Spoel, E. Weckert, and J. Hajdu, *Nature (London)* **406**, 752 (2000).
 - [5] K. J. Gaffney and H. N. Chapman, *Science* **316**, 1444 (2007).
 - [6] S. P. Hau-Riege, R. A. London, and A. Szoke, *Phys. Rev. E* **69**, 051906 (2004).
 - [7] H. M. Quiney and K. A. Nugent, *Nature Phys.* **7**, 142 (2011).
 - [8] U. Saalmann and J. M. Rost, *Phys. Rev. Lett.* **89**, 143401 (2002).
 - [9] V. Averbukh, U. Saalmann, and J. M. Rost, *Phys. Rev. Lett.* **104**, 233002 (2010).
 - [10] G. Wentzel, *Z. Phys.* **43**, 524 (1927).
 - [11] J. L. Campbell and T. Papp, *At. Data Nucl. Data Tables* **77**, 1 (2001).

- [12] P. M. Morse and H. Feshbach, *Methods of Theoretical Physics* (McGraw-Hill, New York, 1953).
- [13] F. Bloch, *Phys. Rev.* **48**, 187 (1935).
- [14] V. Averbukh and L. S. Cederbaum, *J. Chem. Phys.* **123**, 204107 (2005).
- [15] U. Fano, *Phys. Rev.* **124**, 1866 (1961).
- [16] J. Schirmer, L. S. Cederbaum, and O. Walter, *Phys. Rev. A* **28**, 1237 (1983); L. S. Cederbaum, in *Encyclopedia of Computational Chemistry*, edited by P. v. R. Schleyer *et al.* (Wiley, New York, 1998).
- [17] P. Langhoff, *Chem. Phys. Lett.* **22**, 60 (1973); P. W. Langhoff, C. T. Corcoran, J. S. Sims, F. Weinhold, and R. M. Glover, *Phys. Rev. A* **14**, 1042 (1976); P. Langhoff, in *Electron-Molecule and Photon-Molecule Collisions*, edited by T. Rescigno, V. McKoy, and B. Schneider (Plenum, New York, 1979), p. 183; A. U. Hazi, in *Electron-Molecule and Photon-Molecule Collisions*, edited by T. Rescigno, V. McKoy, and B. Schneider (Plenum, New York, 1979), p. 281.
- [18] P. M. W. Gill and L. Radom, *Chem. Phys. Lett.* **147**, 213 (1988).
- [19] G. Karlström, R. Lindh, P.-Å. Malmqvist, B. O. Roos, U. Ryde, V. Veryazov, P.-O. Widmark, M. Cossi, B. Schimmelpfennig, P. Neogrady, and L. Seijo, *Comput. Mater. Sci.* **28**, 222 (2003).
- [20] K. L. Schuchardt *et al.*, *J. Chem. Inf. Model.* **47**, 1045 (2007).
- [21] K. Kaufmann, W. Baumeister, and M. Jungen, *J. Phys. B* **22**, 2223 (1989).
- [22] D. L. Walters and C. P. Bhalla, *Phys. Rev. A* **4**, 2164 (1971). Much larger measured Mg $2p$ widths, e.g., in W. Mehlhorn, B. Breukmann, and D. Hausmann, *Phys. Scr.* **16**, 177 (1977), probably originate from the instrumental resolution.
- [23] A. G. Kochur, D. Petrini, and E. P. da Silva, *Astron. Astrophys.* **365**, 248 (2001).
- [24] J. Breidbach and L. S. Cederbaum, *J. Chem. Phys.* **118**, 3983 (2003).
- [25] P. Kolorenč and V. Averbukh, *J. Chem. Phys.* **135**, 134314 (2011).
- [26] L. S. Cederbaum, J. Zobeley, and F. Tarantelli, *Phys. Rev. Lett.* **79**, 4778 (1997); V. Averbukh, Ph. V. Demekhin, P. Kolorenč, S. Scheit, S. D. Stoychev, A. I. Kuleff, Y.-C. Chiang, K. Gokhberg, S. Kopelke, N. Sisourat, and L. S. Cederbaum, *J. Electron Spectrosc. Relat. Phenom.* **183**, 36 (2011).
- [27] T. Jahnke, H. Sann, T. Havermeier, K. Kreidi, C. Stuck, M. Meckel, M. Schöffler, N. Neumann, R. Wallauer, S. Voss, A. Czasch, O. Jagutzki, A. Malakzadeh, F. Afaneh, Th. Weber, H. Schmidt-Böcking, and R. Dörner, *Nature Phys.* **6**, 139 (2010); M. Mucke, M. Braune, S. Barth, M. Förstel, T. Lischke, V. Ulrich, T. Arion, U. Becker, A. Bradshaw, and U. Hergenbahn, *ibid.* **6**, 143 (2010); I. B. Müller and L. S. Cederbaum, *J. Chem. Phys.* **122**, 094305 (2005).